LA-UR-03-3205
Approved for public release; distribution is unlimited.

Title: **Neutron Reactions on ^{232}U and ^{234}U: Analysis and Evaluation**

Author(s): Phillip G. Young, Mark B. Chadwick, R. E. MacFarlane, and Patrick Talou

Submitted to:

http://lib-www.lanl.gov/cgi-bin/getfile?00852318.pdf

Neutron Reactions on ^{232}U and ^{234}U: Analysis and Evaluation

Phillip G. Young, Mark B. Chadwick, R. E. MacFarlane, and Patrick Talou

ABSTRACT

We have completed analyses of neutron cross sections for ^{232}U and ^{234}U for incident neutron energies between 1 keV and 30 MeV. We combined the results of this analysis with existing ENDF/B-VI resonance-region evaluations to produce new ENDF-formatted data files spanning the incident neutron energy range from 10^{-5} eV to 30 MeV. It was necessary to modify the ENDF/B-VI ^{234}U evaluation in the unresolved resonance region to improve agreement with more recent experimental data. In this report we discuss our theoretical analysis and evaluation of the data and present comparisons with experimental results and other evaluations.

INTRODUCTION

We have completed new evaluations of the neutron cross sections of ^{232}U and ^{234}U over the incident energy range from 10^{-5} eV to 30 MeV. This work is part of a systematic analysis of nuclear reaction data on uranium isotopes from A = 232 to 241 for NW programs. To date, we have provided new evaluated neutron data files for A = 232, 233, 234, 235, 237, 238, 239, 241, all of which cover the neutron energy range 10^{-5} eV to 30 MeV.

The natural abundance of ^{234}U is only 0.0054%; ^{232}U does not occur appreciably in nature. As a result the amount of experimental data available for evaluation of these nuclei is very small. Reasonable experimental databases above 1 keV are only available for fission cross sections, although we were able to make use of some radiative capture data at lower energies. Our approach to evaluating the ^{232}U and ^{234}U cross sections is to perform a theoretical analysis that is optimized to the available fission cross section data and then to utilize the theoretical analysis to calculate unmeasured quantities.

We obtained experimental data from the EXFOR/CSISRS database at the National Nuclear Data Center at Brookhaven National Laboratory. Most of the ^{232}U and ^{234}U fission cross-section data are in the form of ratios to the well known ^{235}U fission cross section. All fission ratios relative to ^{235}U were converted to absolute cross sections using a modification of the ENDF/B-VI standard fission cross section for ^{235}U, described below.

The theoretical analysis involves coupled-channels optical model and Hauser-Feshbach/statistical plus preequilibrium theory calculations. A reliable optical model potential is particularly important for an analysis such as this. Not only are optical model calculations needed for determining neutron total cross sections, elastic and inelastic scattering cross sections and angular distributions, they are required for obtaining neutron transmission coefficients for the reaction theory calculations. As part of our analysis, we assessed several optical model potentials before proceeding with the reaction theory calculations and data evaluation. The optical model and reaction theory analyses are described below.

Our theoretical analysis covers the incident neutron energy range from 1 keV to 30 MeV. At lower energies we combine our results with the ENDF/B-VI evaluations[1, 2] of the resolved and unresolved resonance regions, so that the complete, ENDF-6 formatted evaluations cover the energy range from 10^{-5} eV to 30 MeV. In the course of melding our evaluations at higher energies with the resonance region evaluations, we found it necessary to modify the ENDF/B-VI evaluation of unresolved resonance parameters for ^{234}U in order to enhance agreement with experimental data.[3]

THEORETICAL ANALYSIS

The primary goal of the theoretical analysis is to provide a consistent set of data for all reactions over the energy range 1 keV to 30 MeV. Because available experimental data is limited mainly to fission cross sections, the theoretical analysis was used to provide the total, elastic, inelastic, (n,2n), (n,3n) and (n,4n) cross sections, together with a smooth representation of the (n,f) and (n,γ) cross sections, and the angular and energy distributions of secondary neutrons. To accomplish this, an assessment of a suitable coupled-channels optical model potential was carried out, and then a preliminary reaction theory analysis was performed utilizing Hauser-Feshbach, statistical, preequilibrium, direct reaction, level density, and gamma-ray strength function models.

Optical Model Analysis

Because of the lack of neutron total and scattering experimental data for ^{232}U and ^{234}U, we adopted the approach of trying to develop an optical model for these nuclei using theory and systematics to infer potentials from those derived for ^{238}U, for which there exist many measurements. We investigated coupled-channels ^{238}U potentials by Madland and Young,[4] several potentials from Haouat et al.[5] and Lagrange[6] at Bruyères-le-Châtel (BRC), and two potentials by Young and Arthur.[7, 8] It was necessary to make modifications to both the Madland and the BRC potentials in order to apply them in the present analysis.

The BRC actinide potentials were derived for individual isotopes based on coupled-channels optical model analyses of experimental data up to a few MeV for ^{230}Th, ^{232}Th, ^{234}U, ^{235}U, ^{238}U, ^{239}Pu, and ^{242}Pu. We generalized these results for individual isotopes into an isospin-dependent potential, with separate formulations of the imaginary surface-derivative potential, W_d, for even- and odd-A nuclei. This separation was done primarily because the values of W_d from the BRC analyses of ^{235}U and ^{238}U differ significantly. Because these potentials were derived from experimental data below a few MeV, we extended them to higher energies by assuming that W_d saturates at 10 MeV and remains constant thereafter.

The original Madland and Young potential was derived for the energy range 0.01 to 10 MeV, with isospin terms obtained by fitting data for several actinides. To extend the range of validity to higher energies, we again assumed a constant imaginary surface potential well depth above 10 MeV. For the Young and Arthur potential, we assumed isospin dependence similar to BRC potential.

We performed detailed comparisons of these potentials by calculating total cross sections and elastic and inelastic scattering angular distributions and comparing the results with experimental data. The details of these comparisons are summarized in a previous internal document.[9] Our overall conclusion was that a new coupled-channels optical model analysis spanning the energy range 10 keV to 30 MeV would be very useful. For the present analysis, however, we chose to utilize our modified version of the BRC potentials. This potential is given in Table 1. For completeness, we also include the odd-A potential, which was not needed in our present analysis.

The optical model calculations were performed with the 1996 version of the ECIS coupled-channels optical model code developed by Raynal.[10] The calculations include coupling of the lowest three members of the ground state rotational band of ^{232}U and ^{234}U to obtain direct components for (n,n') cross sections and angular distributions to the first two excited states. This coupling was also used to generate the neutron transmission coefficients for the reaction theory calculations, described below. A special calculation coupling four states was run to determine the direct (n,n') components for the 3rd excited states. The rotational bands for ^{232}U and ^{234}U are given in Table 2.

Table 1. Optical model potential used in the evaluation of n + ^{232}U and n + ^{234}U reactions. Energies are in MeV, radii and diffusivities are in fm, E_n is the incident neutron energy, and η = (N-Z)/A, where N, Z, and A are the neutron, proton, and atomic mass numbers for the target nucleus.

$V_V = 50.328 - 0.30E_n - 18.194\eta$	$0 \le E_n \le 30$	$r_V = 1.26$	$a_V = 0.63$
$W_V = 0$	$0 \le E_n \le 30$	$r_V = 1.26$	$a_V = 0.52$
$V_{SO} = 6.20$	$0 \le E_n \le 30$	$r_{SO} = 1.12$	$a_{SO} = 0.47$
EVEN A			
$W_D = 5.642 + 0.4E_n - 9\eta$	$0 \le E_n \le 10$	$r_D = 1.26$	$a_D = 0.52$
$= 9.642 - 9\eta$	$10 \le E_n \le 30$		
ODD A			
$W_D = 5.253 + 0.4E_n - 9\eta$	$0 \le E_n \le 10$	$r_D = 1.26$	$a_D = 0.52$
$= 9.253 - 9\eta$	$10 \le E_n \le 30$		

Deformation parameters: ^{232}U $\beta_2 = 0.190$ $\beta_4 = 0.076$
^{234}U $\beta_2 = 0.197$ $\beta_4 = 0.071$

Table 2. ^{232}U and ^{234}U ground-state rotational bands. Only the lowest three states were included in the optical model calculations.

^{232}U			^{234}U		
E_x (MeV)	J	π	E_x (MeV)	J	π
0.	0	+1	0.	0	+1
0.047572	2	+1	0.043498	2	+1
0.15657	4	+1	0.143351	4	+1
0.3226	6	+1	0.296071	6	+1
0.5410	8	+1	0.49704	8	+1
0.8058	10	+1	0.7412	10	+1
1.1115	12	+1	1.0238	12	+1

Reaction Theory Calculations

The Hauser-Feshbach statistical calculations were performed with the COMNUC[11] and GNASH[12] codes. Both codes include a double-humped fission barrier model, using uncoupled oscillators for the barrier representation in GNASH and coupled or uncoupled oscillators in COMNUC, as described by Arthur.[13] The COMNUC calculations include the possibility of width-fluctuation corrections and corrections for class II fluctuations, which are needed at lower energies, whereas GNASH provides the preequilibrium corrections that are required at higher energies. Accordingly, COMNUC was used in the calculations below about 0.5 MeV and GNASH was employed at higher energies using two uncoupled oscillators in the fission calculations.

Each compound nucleus formed in the calculations is permitted to decay through the fission channel, by neutron emission, and by gamma-ray emission. Neutron transmission coefficients for the Hauser-Feshbach calculations are obtained from the coupled-channel optical model calculations with ECIS. Gamma ray transmission coefficients are obtained from gamma-ray strength functions calculated with the generalized Lorentzian model of Kopecky and Uhl.[14] Transmission coefficients for fission are calculated from the fission model detailed in ref. 12.

Gilbert and Cameron[15] phenomenological level density functions were used to represent continuum levels at ground-state deformations, appropriately matched to available experimental structure data at lower excitation energies. Multiplicative factors were applied to the level density functions to account for enhancements in the fission transition state densities at the fission barriers due to increased asymmetry conditions, and the continuum level densities were matched to the discrete fission transition states at each barrier. The discrete fission transition state spectra were calculated from bandhead information taken from calculations and compilations by Britt[16]

^{232}U DATA EVALUATION AND RESULTS

Resonance Region

The resolved and unresolved resonance region data in the existing version of the ENDF/B-VI (MOD 2) evaluation[1] for ^{232}U are adopted in the present work. In that evaluation, the resolved resonances are represented by Reich-Moore parameters obtained from Mughabghab[17] and cover the incident neutron energy range from 10^{-5} to 194 eV. The unresolved resonance region parameters also utilize Mughabghab's data, with D_0 = 4.60 eV, S_0 = 1.2 x 10^{-4}, Γ_γ = 40 meV, and R_{scat} = 9.8 fm. The unresolved resonance region extends from 194 eV to 2 keV. The calculated thermal cross sections and resonance integrals are given in Table 3.

Table 3. Calculated 2200 m/s cross sections and resonance integrals from the present ^{241}U evaluation using ENDF/B-VI resonance parameters.

Reaction	Cross Section (barns)	Resonance Integral (barns-eV)
Total	162.77	
Elastic	10.79	
Fission	76.77	309.8
Capture	75.21	161.9

Smooth Cross Sections

Above the unresolved resonance region (2 keV), we obtain new evaluations for the neutron total, elastic, (n,n'), (n,2n), (n,3n), (n,4n), (n,f), (n,nf), (n,2nf), (n,3nf), and (n,γ) cross sections. In this section we compare our results with several existing evaluations: the initial ENDF/B-VI (MOD 1)[18] evaluation, which is actually ENDF/B-V.2; the existing ENDF/B-VI (MOD 2)[1] evaluation; and a recent evaluation by Maslov.[19] It should be noted that the ENDF/B-VI (MOD 2) evaluation was taken from the JENDL-3.2 evaluation[20] with minor updating and modification. It might be further noted that the JENDL-3.3 evaluation is based on JENDL-3.2, and the JEF-3.0 evaluation is ENDF/B-V.2.

Our evaluated ^{232}U(n,2n) cross section, which is taken directly from our GNASH analysis, is compared to the other evaluations in Fig. 1. The present result is lower than the other evaluations and is closest to the recent Maslov evaluation. Note that the original ENDF/B-VI (MOD 1) evaluation is a factor of 10-30 higher than the other evaluations.

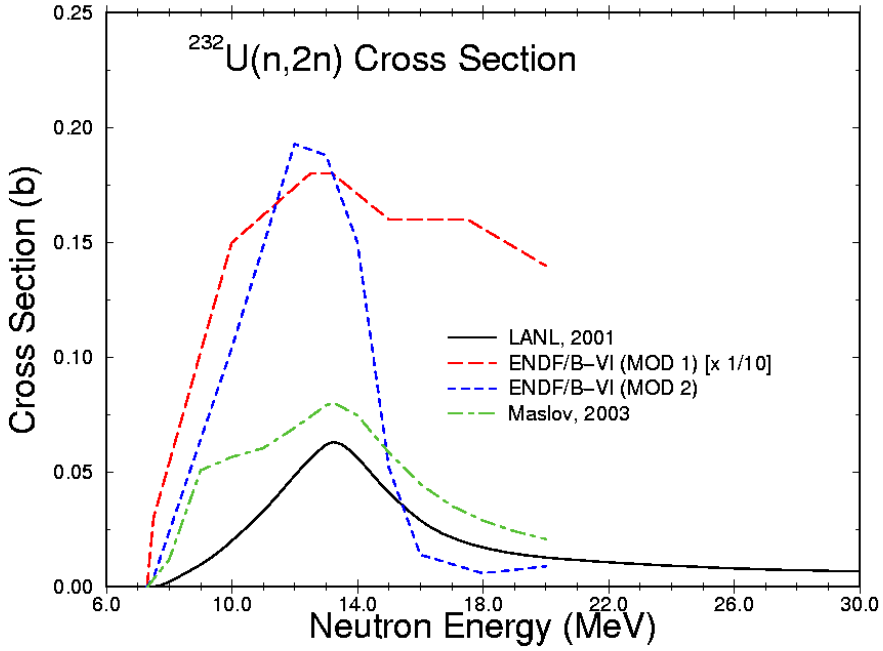

Fig. 1. Evaluated ^{232}U(n,2n) cross section from threshold to 30 MeV.

Our evaluated ^{232}U(n,3n) cross section, which also is taken directly from our GNASH calculations, is compared to the other evaluations in Fig. 2. In this case again our result is lower than the other evaluations but is close in shape to the Maslov work. The ENDF/B-VI (MOD 1) evaluation is a factor of 100 higher than the other evaluations. It might be noted that the (n,5n) cross section, which thresholds at 26.9 MeV, is lumped with the (n,4n) cross section (MT = 37) because there is no MT number in the ENDF-6 format for (n,5n) reactions.

Direct components for the (n,n') reactions to the first three excited states of ^{232}U (MT = 51-53) were obtained from the ECIS96 calculations. Compound-nucleus contributions for all discrete (n,n') excitation cross sections (MT=51-90) were obtained from the GNASH calculations, as was the (n,n'continuum) cross section (MT=91). Direct cross section components for MT = 54-90 were taken from the ENDF/B-VI (MOD 5) evaluation[21] of ^{238}U. (The ^{238}U direct cross sections are based on ECIS96 calculations, normalized to be consistent with ^{238}U (n,xn) neutron spectrum measurements near 14 MeV.)

The ^{232}U inelastic cross section that results from summing all the individual (n,n') components is compared to the other evaluations in Fig. 3. Again, the present result is close to the recent Maslov evaluation. The very low (n,n') cross sections above 10-12 MeV in the ENDF/B-VI evaluations are nonphysical and reflect the absence of direct reactions in those evaluations.

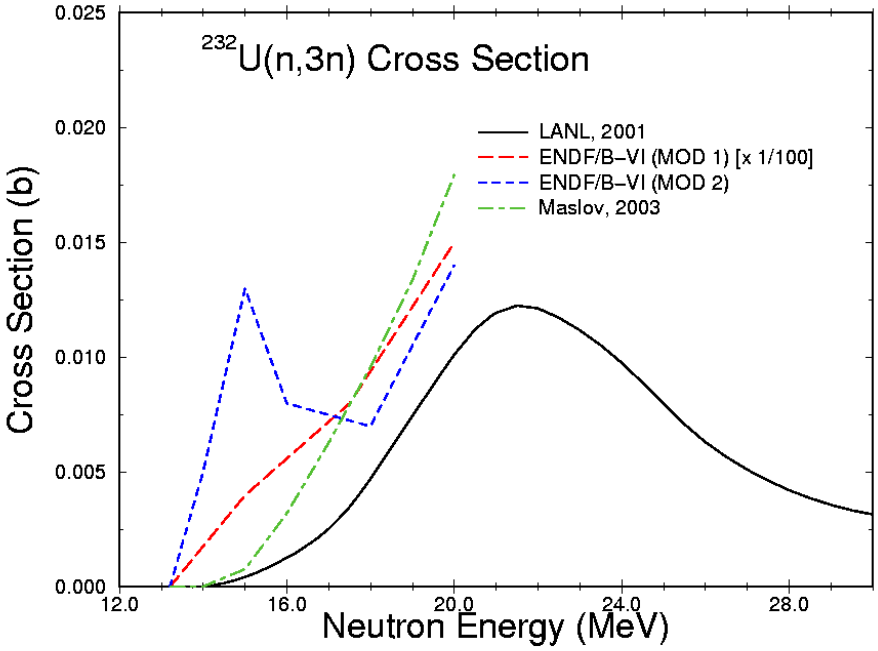

Fig. 2. Evaluated ^{232}U(n,3n) cross section from threshold to 30 MeV.

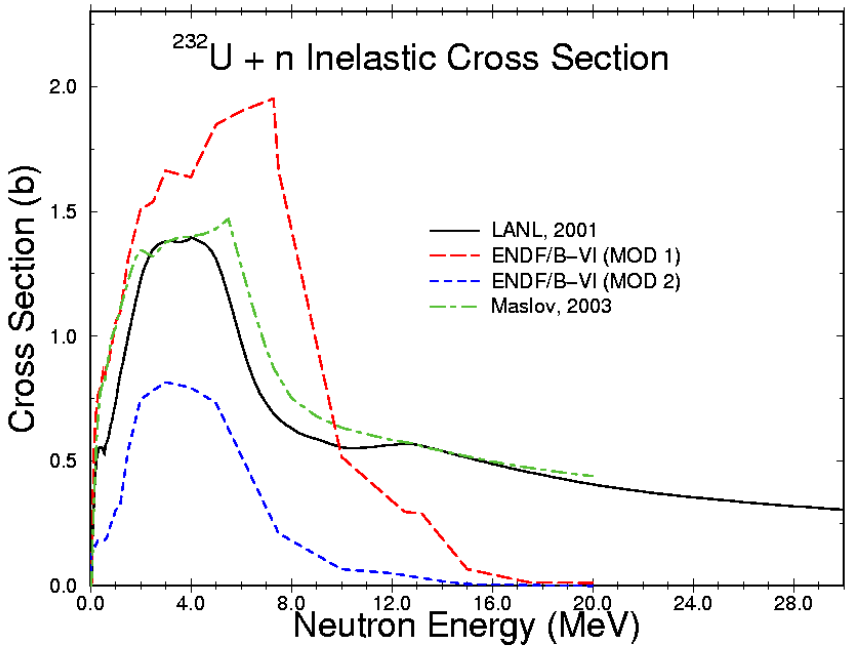

Fig. 3. Evaluated total ^{232}U(n,n') cross section from threshold to 30 MeV.

The total fission cross section (MT = 18) in our evaluation at lower energies is based on the experimental data of Fursov[22] and follows closely the ENDF/B-VI (MOD 2) evaluation[1] to a neutron energy of 7 MeV. For the energy range 7 – 30 MeV, the (n,f) cross section is taken from the GNASH analysis. Our results below 4 MeV are compared to the other evaluations and to our GNASH calculations in Fig. 4. Similarly, in Fig. 5 we show the various evaluations and the calculation from 4 to 30 MeV.

The fission barrier and level density parameters used for the ^{232}U + n GNASH calculations were taken from a combined analysis[9] of uranium target isotopes from A=232 to A=238, and no effort was made to specifically optimize the parameters for ^{232}U. Consequently the match between theory and experiment is somewhat poor below 2 MeV. At higher energies the calculated cross section is satisfactory. The nonphysical value of the fission cross section above 5 MeV [as well as the (n,xn) cross sections] from the original ENDF/B-VI (MOD 1) evaluation reflects the fact that the MOD 1 evaluation, which was completed in 1977, was directed primarily at fission reactor applications.

We also include in our evaluation tabulations for the (n,nf), (n,2nf), (n,3nf) and (n,4nf) cross sections with the smooth cross sections in MF = 3. These were taken directly from the GNASH analysis above 7 MeV and at lower energies were determined by multiplying the MT=18 cross section by the appropriate ratios determined from the GNASH calculations.

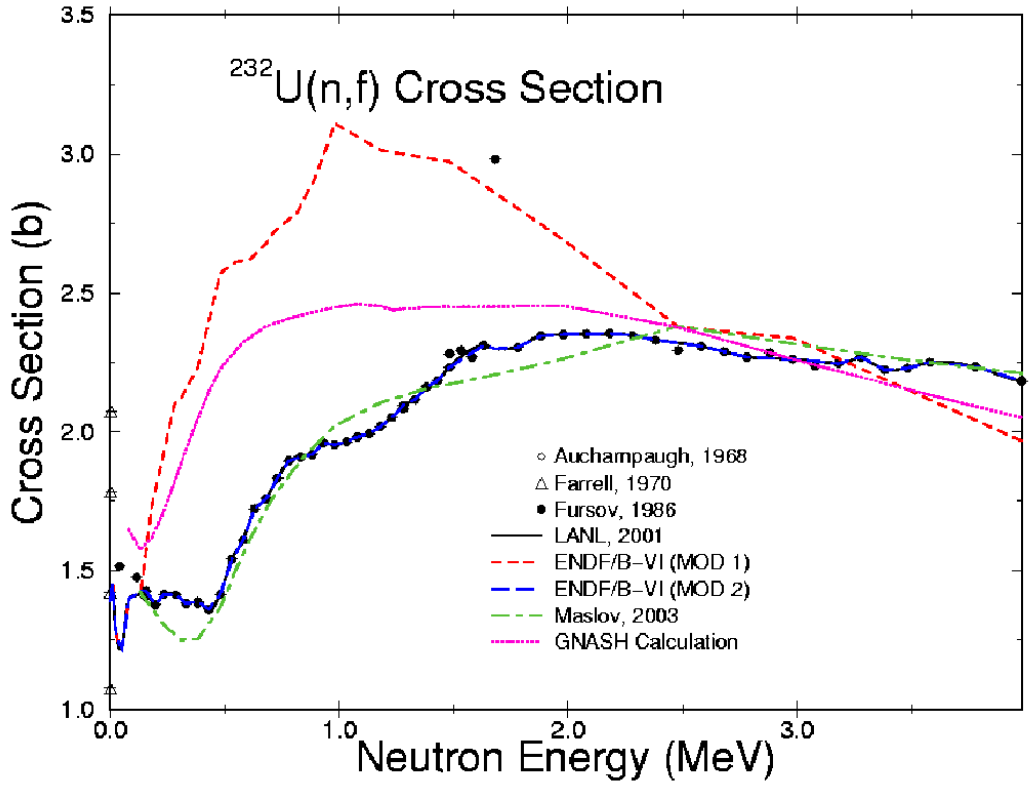

Fig. 4. Evaluated and measured ^{232}U(n,f) cross section from 2 keV to 4 MeV.

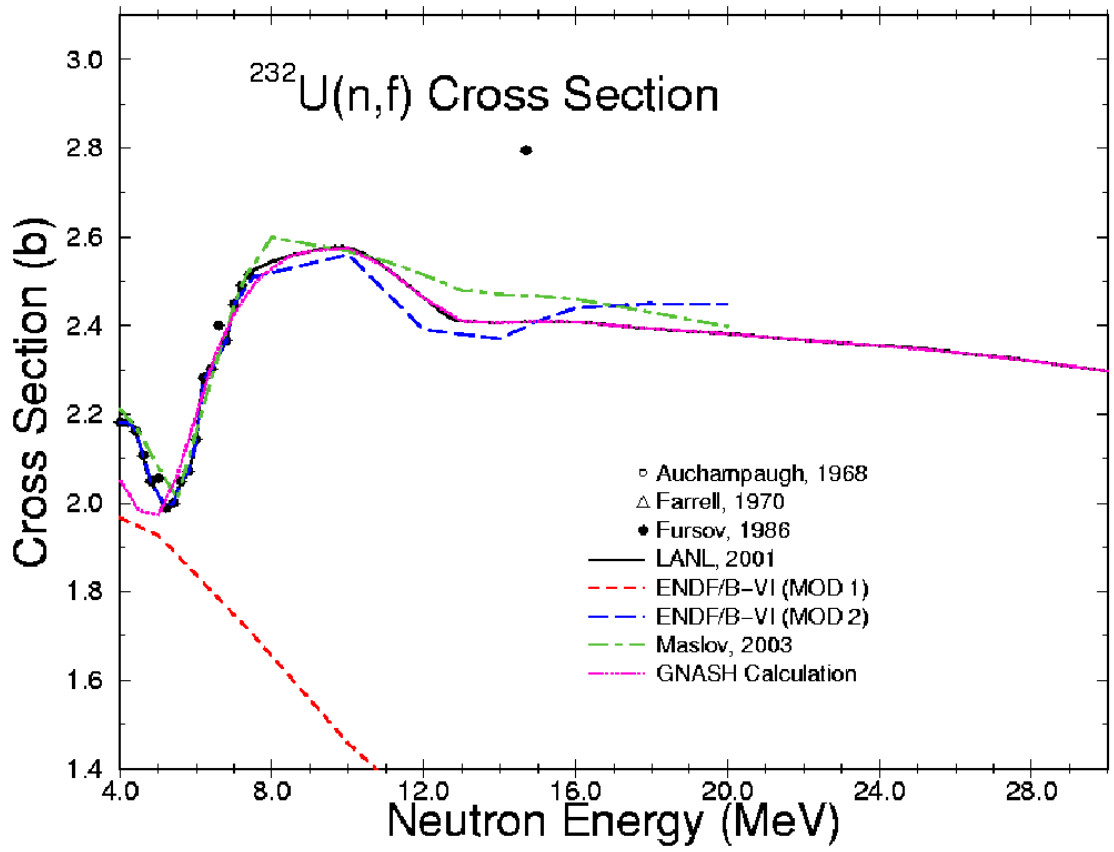

Fig. 5. Evaluated and measured ^{232}U(n,f) cross sections from 4 to 30 MeV.

Our evaluated ^{232}U(n,γ) cross section, which is based completely on the GNASH analysis, is compared with the other evaluations in Fig. 6. The total nonelastic cross section that results from summing all the individual reactions is shown between 0.001 and 2 MeV in Fig. 7 and between 2 and 30 MeV in Fig. 8. For comparison, the reaction cross section that results from our coupled-channels optical model calculations is included in Figs. 7 and 8. Because the reaction cross section includes the compound elastic cross section, it is significantly higher than the nonelastic cross sections at lower energies. Above 2 MeV, the compound elastic is very small and the reaction cross section essentially equals the nonelastic cross section.

The neutron total cross section (MT = 1) from 10 keV to 30 MeV is based on the ECIS96 coupled channels optical model calculations. Between 2 and 10 keV, the optical model results are smoothly joined to the ENDF/B-VI (MOD 2) cross section. These results are compared to the other evaluations between 0.001 and 2 MeV in Fig. 9 and between 2 and 30 MeV in Fig. 10. The vertical breaks in the evaluated cross sections in Fig. 9 (as well as in Figs. 6 and 7) mark the upper energy of the unresolved resonance regions in the evaluations. Our evaluated total cross section is quite similar to those given in ENDF/B-VI (MOD 2) and Maslov's evaluation.

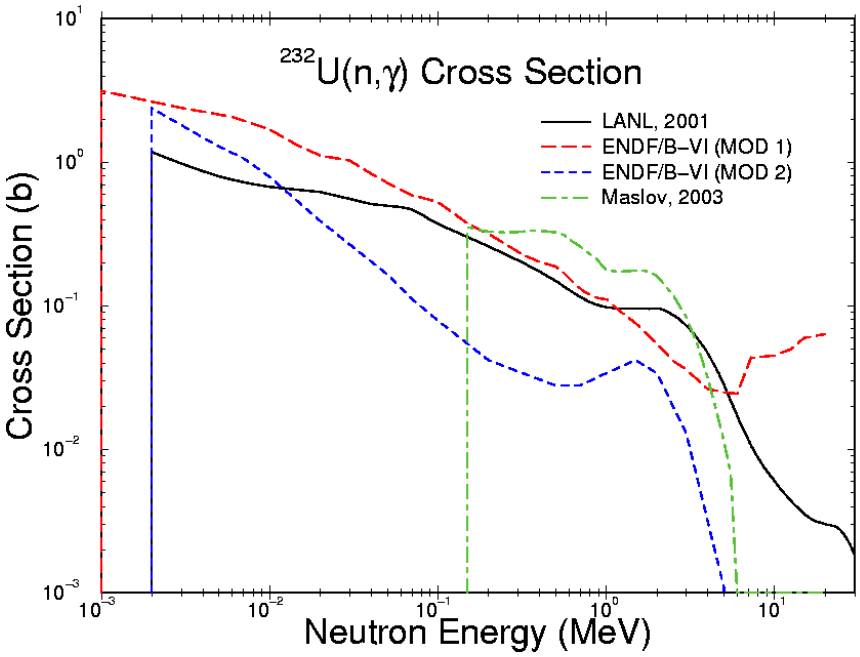

Fig. 6. Evaluated ^{232}U(n,γ) cross section from 0.001 to 30 MeV.

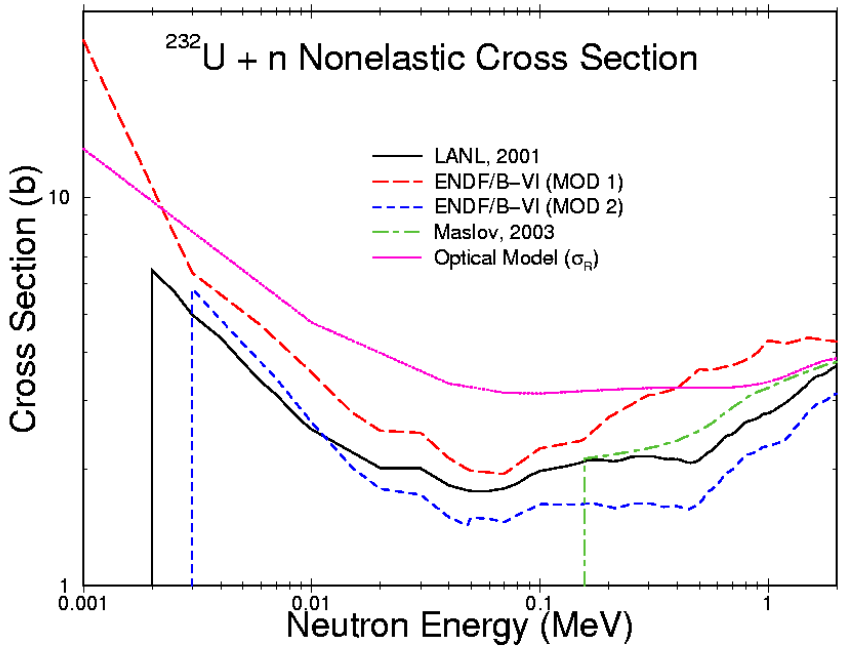

Fig. 7. Evaluated ^{232}U + n nonelastic cross section from 0.001 to 2 MeV. The optical model reaction cross section is included for comparison.

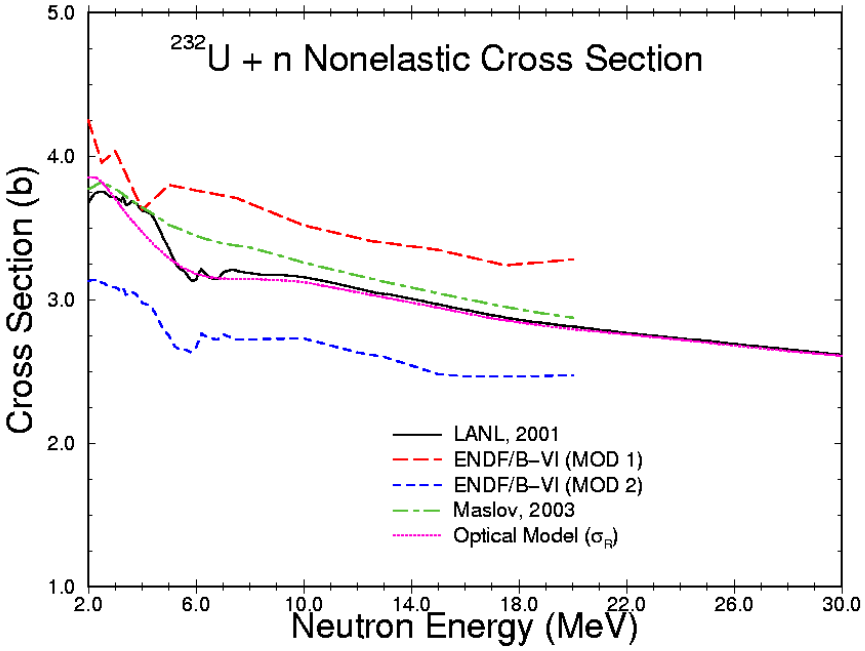

Fig. 8. Evaluated ^{232}U + n nonelastic cross section from 2 to 30 MeV. The optical model reaction cross section is included for comparison.

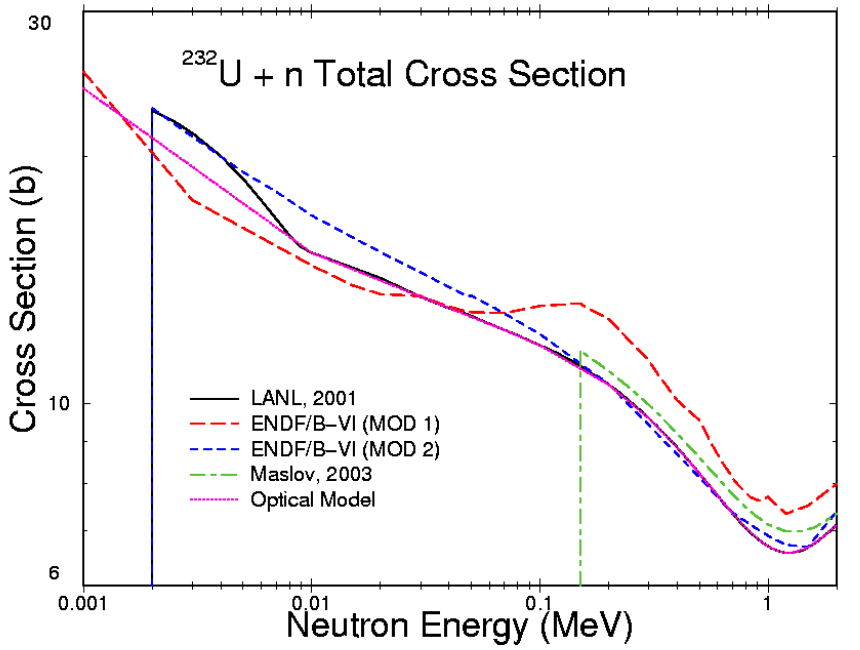

Fig. 9. Evaluated and calculated ^{232}U + n total cross section from 0.001 to 2 MeV.

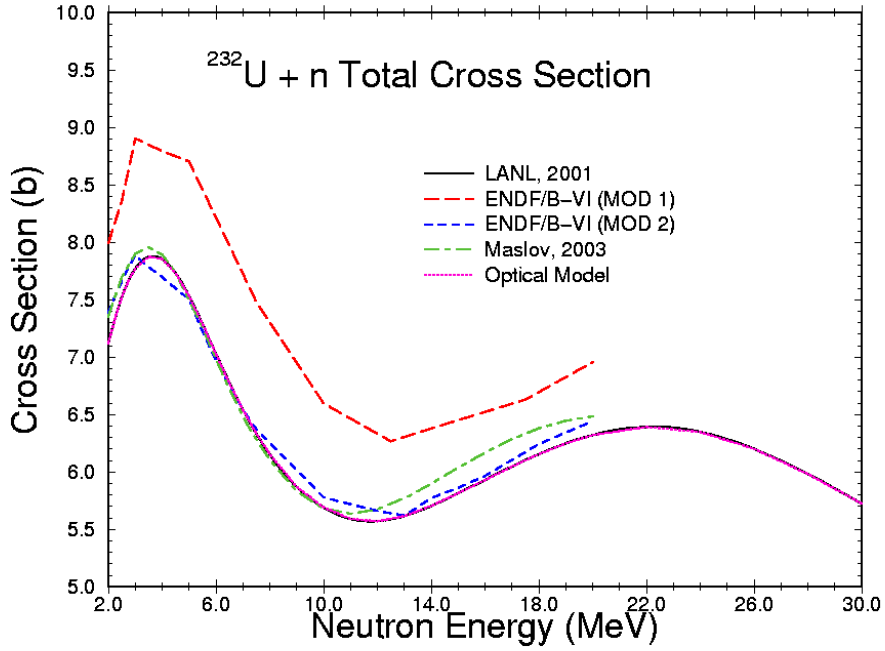

Fig. 10. Evaluated and calculated ^{232}U + n total cross section from 2 to 30 MeV.

We obtained the elastic cross section by subtracting the nonelastic cross section from the total cross section. These results are compared to the other evaluations between 0.001 and 2 MeV in Fig. 11 and between 2 and 30 MeV in Fig. 12. We also include the shape elastic cross section from our optical model calculations in the figures. The shape elastic differs from the full elastic cross section by the compound elastic cross section, so it is essentially equivalent to the elastic cross section above ~2 MeV. Because we utilized experimental data for the fission cross section and included (n,n') direct cross sections from our ^{238}U analysis, our evaluated elastic cross section does not exactly equal the optical model values. As seen in Fig.12, however, the two results are very close above 2 MeV.

Neutron Angular Distributions

The elastic scattering angular distributions were determined by combining the compound elastic contribution from COMNUC calculations with the shape elastic contribution calculated with ECIS96 from the coupled-channels optical model potential. Below 10 MeV, Legendre polynomials are used to represent the angular distributions. Above 10 MeV, the angular distributions are tabulated to prevent problems with the limitation on the maximum order of Legendre expansions permitted under ENDF-6 rules.

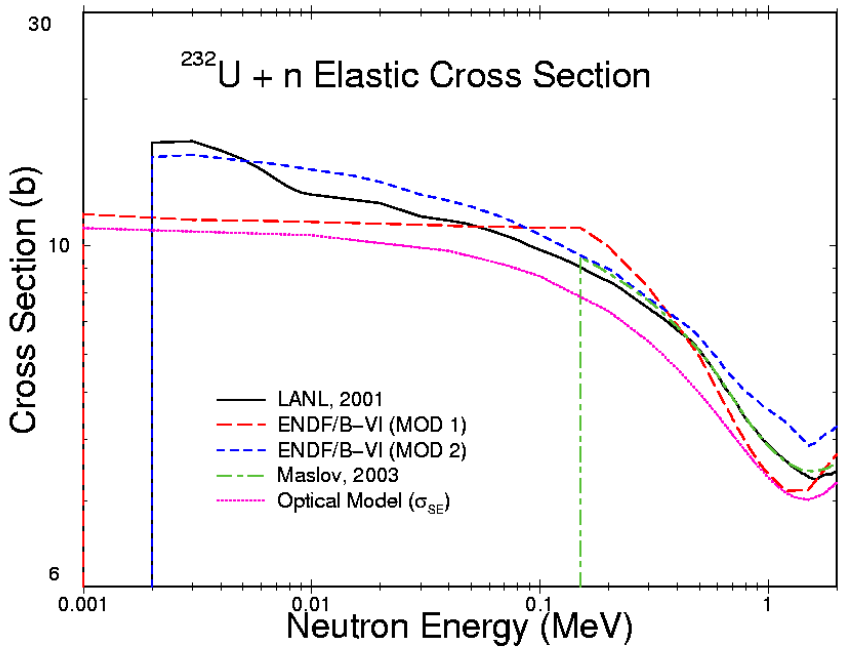

Fig. 11. Evaluated and calculated ^{232}U + n elastic cross section from 0.001 to 2 MeV.

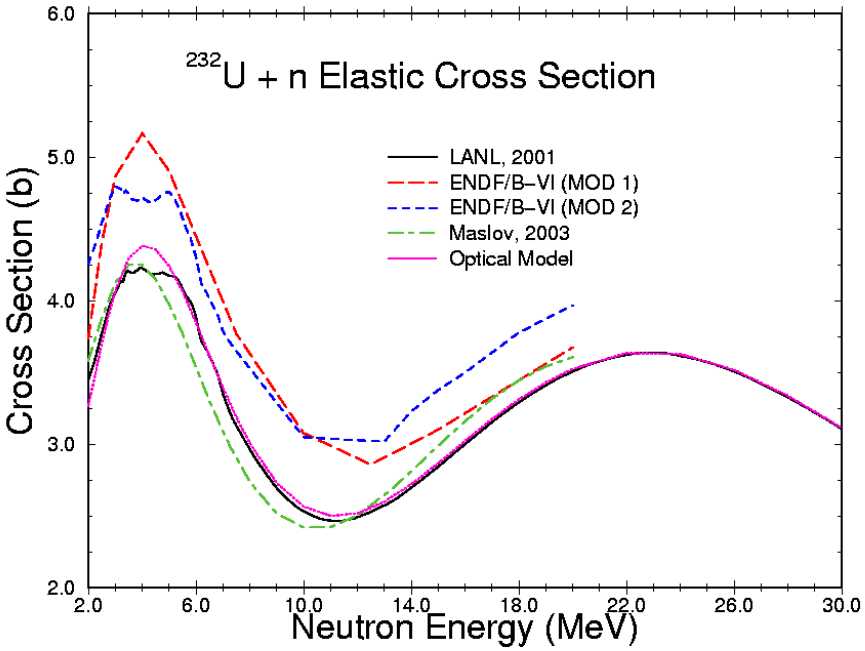

Fig. 12. Evaluated and calculated ^{232}U + n elastic cross section from 2 to 30 MeV.

The discrete ^{232}U (n,n') angular distributions for MT=51-53 were also determined by combining compound nucleus contributions from the COMNUC analysis with direct reaction contributions from the coupled-channels optical calculations. For MT=54-90 preequilibrium shapes were used for the angular distributions. Legendre expansions were used for all the (n,n') angular distributions. Neutrons from fission reactions (MT=18) are given in the evaluation as isotropic.

Energy-Angle Distributions

Energy-angle distributions in MF=6 are used to represent neutrons from (n,n'continuum), (n,2n), (n,3n), and (n,4n) reactions, corresponding to MT=91, 16, 17, and 37, respectively. The energy distributions were obtained from the GNASH analysis. The angular distributions are given using Kalbach systematics[23] with the LAW=1, LANG=2 Kalbach-Mann option in MF=6.

Fission Neutron Spectra and Prompt Fission Nubar

The fission neutron spectra and prompt nubar in the present evaluation were adopted directly from the ENDF/B-VI (MOD 2) evaluation[1] with linear extrapolation of the data to 30 MeV. Our evaluation of prompt nubar is compared with the other evaluations in Fig. 13. The present results are higher than Maslov's evaluation by approximately 10% in the 10-20 MeV region.

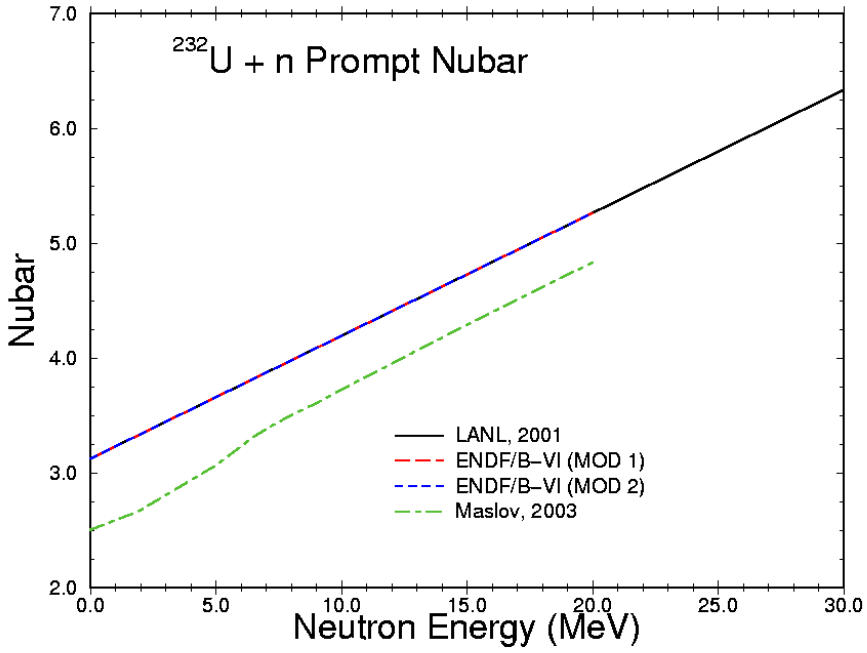

Fig. 13. Evaluated ^{232}U + n prompt fission nubar from 0 to 30 MeV

^{234}U DATA EVALUATION AND RESULTS

Resonance Region

The resolved and unresolved resonance region data in the previous version of the ENDF/B-VI evaluation[2] for ^{234}U are adopted in the present work, with some modification of the unresolved parameters to enhance agreement with experiment. In the ENDF/B-VI evaluation, the resolved resonances are taken from James et al.,[24] with the bound level parameters modified to fit BNL-325 Vol. 1 thermal and resonance integral cross sections. The resolved resonance region covers the incident neutron energy range from 10^{-5} eV to 1.5 keV.

The unresolved resonance region parameters were obtained originally by fitting the averaged (n,f) cross section data of James et al. and ENDF/B-IV radiative capture cross sections from 1.5 to 100 keV. We modified $<\Gamma_\gamma>$ from 25 meV to 37.5 meV in order to improve agreement with the experimental data of Muradyan et al.[3] near the top of the resolved resonance region. The unresolved resonance region extends from 1.5 to 100 keV. The calculated thermal cross sections and resonance integrals are given in Table 4.

Table 4. Calculated 2200 m/s cross sections and resonance integrals from the present ^{234}U evaluation using ENDF/B-VI resonance parameters.

Reaction	Cross Section (barns)	Resonance Integral (barns-eV)
Total	115.802	
Elastic	12.301	
Fission	0.464	6.435
Capture	103.036	659.675

Smooth Cross Sections

Above the unresolved resonance region, new evaluations are given for the neutron total, elastic, (n,n'), (n,2n), (n,3n), (n,4n), (n,f), (n,nf), (n,2nf), (n,3nf), and (n,γ) cross sections. We compare our results with the following evaluations: the existing ENDF/B-VI (MOD 1) evaluation,[2] the JENDL-3.3 evaluation,[25] and a new evaluation by Maslov.[26] It should be mentioned that the ENDF/B-VI (MOD 1) evaluation is a carryover from ENDF/B-V.2 and that the JEF-3.0 evaluation is also taken from ENDF/B-V.2.

As with ^{232}U, the ^{234}U(n,γ) (MT = 102) and the ^{234}U(n,xn) cross sections (MT = 16, 17, 37) for the present evaluation were taken directly from the GNASH calculations.

We compare our evaluated ^{234}U(n,2n) cross section with ENDF/B-VI, JENDL-3.3, and with Maslov's evaluation in Fig. 14. The JENDL-3.3 evaluation is significantly higher than the other evaluations between threshold and 14 MeV. Again, our results are closest to the Maslov evaluation.

Our evaluated ^{234}U(n,3n) cross section is compared to the other evaluations in Fig. 15. Again the (n,5n) cross section, which thresholds at 25.7 MeV, is lumped with the (n,4n) cross section (MT = 37).

As was the case for our ^{232}U evaluation, direct components for the (n,n') reactions to the first three excited states of ^{234}U (MT = 51-53) were obtained from the ECIS96 calculations. Compound-nucleus contributions for all discrete (n,n') excitation cross sections (MT=51-90) were obtained from the GNASH calculations, as was the (n,n'continuum) cross section (MT=91). Direct cross section components for MT = 54-90 were again taken from the ENDF/B-VI (MOD 5) evaluation[21] of ^{238}U.

The ^{234}U inelastic cross section that results from summing all the individual (n,n') components is compared to the other evaluations in Fig. 16. Again, the present result is reasonably close to the recent Maslov evaluation. Both the ENDF/B-VI and the JENDL-3.3 evaluations have significantly lower (n,n') cross sections above 12 MeV compared to our evaluation and to Maslov's evaluation.

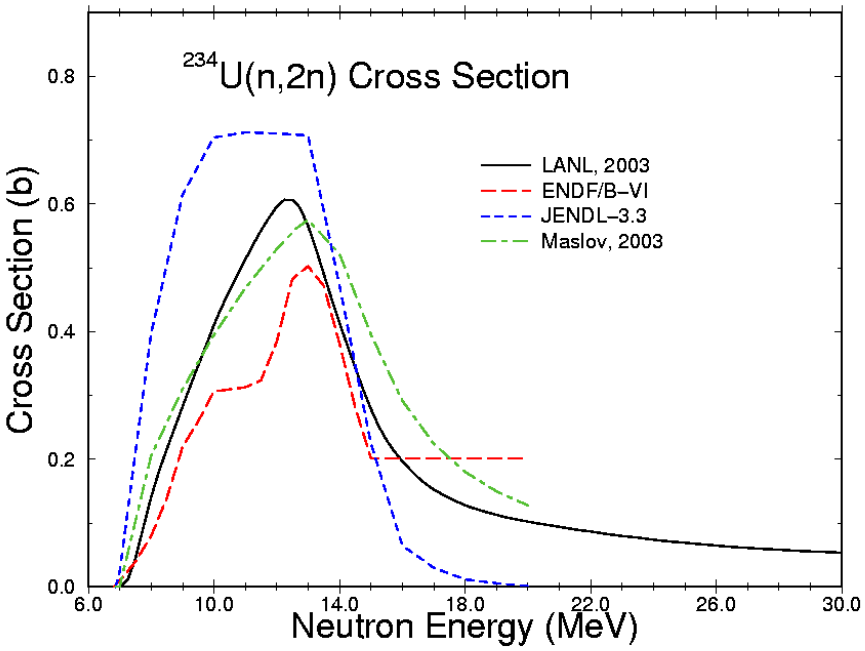

Fig. 14. Evaluated ^{234}U(n,2n) cross section from threshold to 30 MeV.

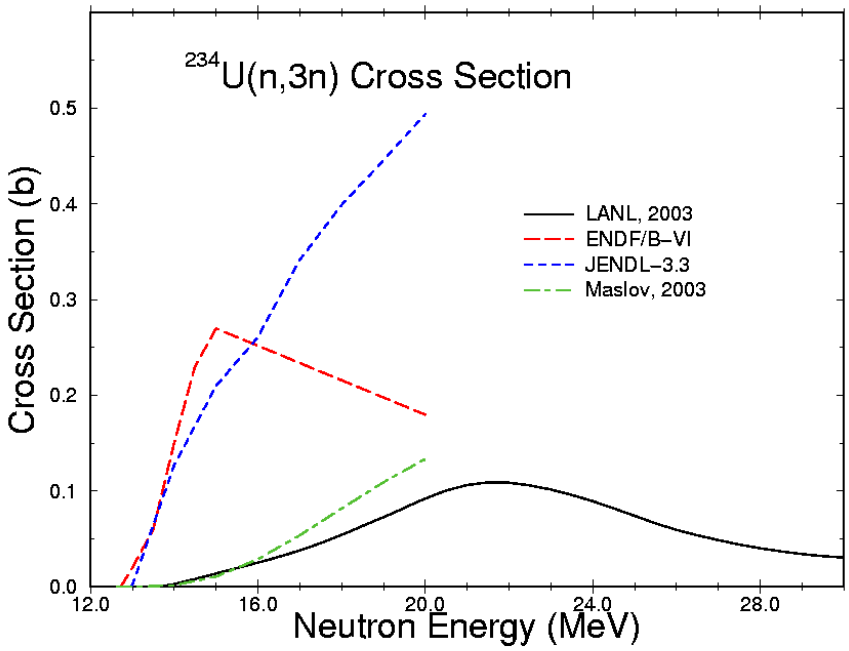

Fig. 15. Evaluated ^{234}U(n,3n) cross section from threshold to 30 MeV.

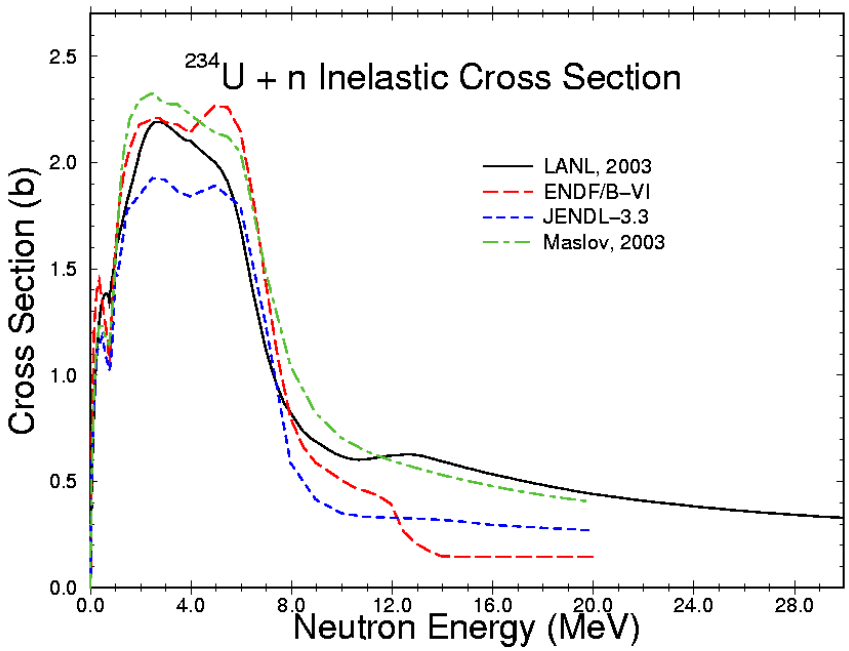

Fig. 16. Evaluated total ^{234}U(n,n') cross section from threshold to 30 MeV.

The fission cross section experimental data for ^{234}U that we utilized are relative to ^{235}U. The ^{234}U ratio measurements were converted to absolute values using a revision of the ENDF/B-VI ^{235}U(n,f) cross section standard by Talou and Young.[27] This revised reference cross section is slightly higher than the Version VI standard in the 1-4 MeV region, and significantly higher above 14 MeV. Above 14 MeV, this reference cross section is taken from the International Atomic Energy Agency (IAEA) revised standard cross section.[28]

The total fission cross section (MT = 18) in our evaluation is based on the experimental data of White et al.[24] at neutron energies below 2 MeV. From 2 to 30 MeV, the evaluation primarily follows the experimental data of Behrens and Carlson.[29] The Behrens data covers most of the energy range of our evaluation and appears reasonably consistent with the measurements of Fursov *et al.*,[30] Meadows,[31] Kanda et al.,[32] and Meadows.[33] Our results below 4 MeV are compared to the other evaluations and to our GNASH calculations in Fig. 17. Similarly, in Fig. 18 we show the various evaluations and the calculation from 4 to 30 MeV.

Similar to the ^{232}U evaluation, the fission barrier and level density parameters used for the ^{234}U + n GNASH calculations were taken from a combined analysis[9] of uranium target isotopes from A=232 to A=238, and no effort was made to specifically optimize the parameters for ^{234}U. Consequently the match between theory and experiment is not optimum at all energies.

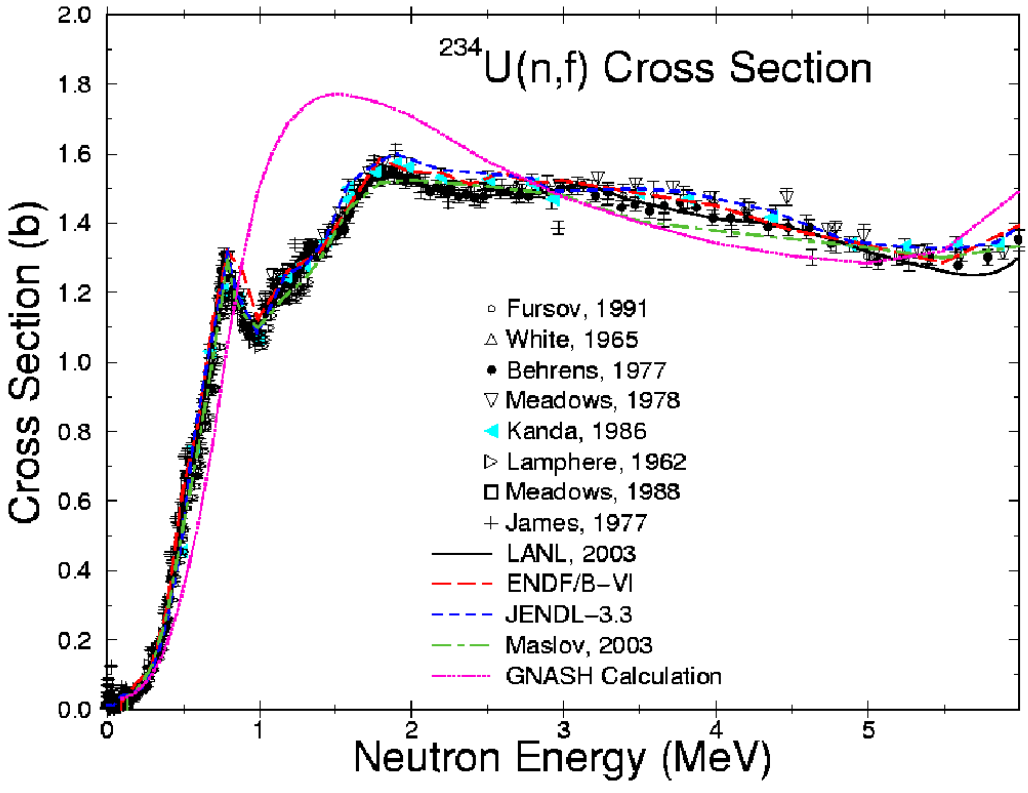

Fig. 17. Evaluated and measured ^{234}U(n,f) cross section from 0 to 6 MeV.

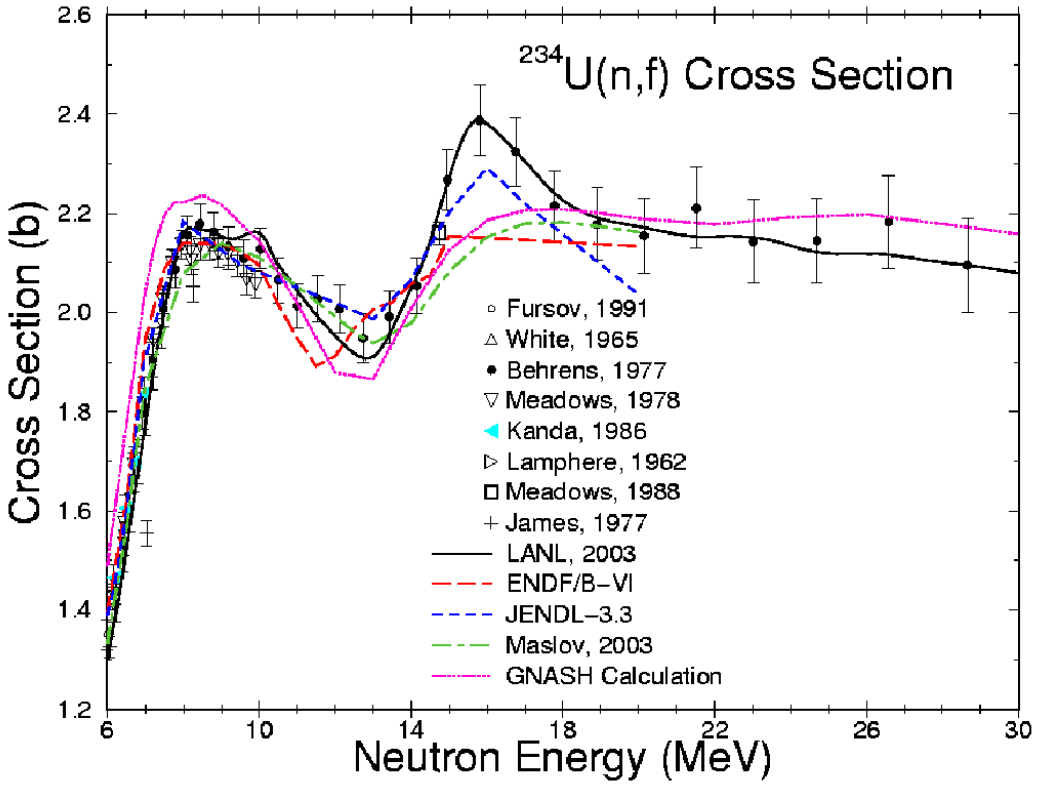

Fig. 18. Evaluated and measured ^{234}U(n,f) cross sections from 6 to 30 MeV.

We include tabulations in our evaluation of the (n,nf), (n,2nf), (n,3nf) and (n,4nf) cross sections with the smooth cross sections in MF = 3. Again, these were taken directly from the GNASH analysis above 7 MeV and at lower energies were determined by multiplying the MT=18 cross section by the appropriate ratios determined from the GNASH calculations.

While most of our effort was directed at the energy range above 1 keV, we did modify $\langle\Gamma_\gamma\rangle$ from 25 meV to 37.5 meV in the unresolved resonance region. This was done to improve agreement with the epithermal ^{234}U(n,γ) cross section data of Muradyan et al.[3] Muradyan's data cover the energy range 4.65 – 2150 eV, which lies mostly in the resolved resonance region of our evaluation but which reaches the unresolved region. The experimental data are compared in Fig. 19 to our evaluation and to ENDF/B-VI. The pointwise evaluations and experimental data are shown in the upper half of Fig. 19, while in the lower half of the figure, the data are compared to our evaluation and to ENDF/B-VI averaged with the NJOY code[34] over the experimental energy groups. Our results are in good agreement with the Muradyan data near the unresolved energy region boundary (1500 eV). At lower energies, however, the resolved resonance region evaluation mostly underpredicts the measurements.

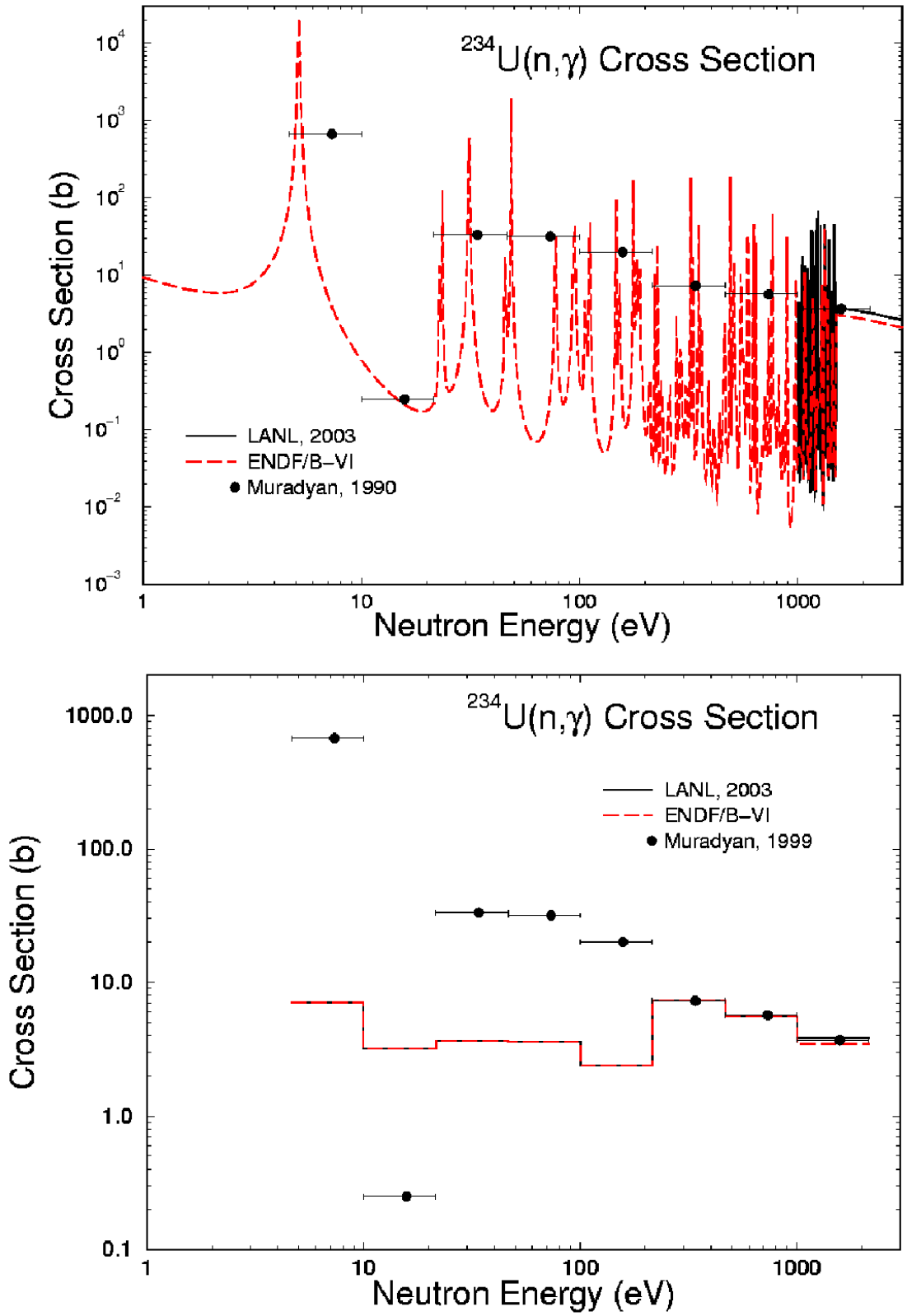

Fig. 19. Evaluated ^{234}U(n,γ) cross sections compared to Muradyan et al.[3] experimental data. The upper half shows the pointwise evaluations; the lower half compares group-averaged evaluation values with the data over same energy bins as the measurement.

Above 100 keV, the (n,γ) cross section is based on our GNASH calculation, normalized to match the value from the unresolved resonance region at 100 keV. To accomplish this, it was necessary to use a value of $2\pi\Gamma_\gamma/d_0$ that is two standard deviations higher than the value inferred from resonance data. These results are shown in Fig. 20, together with the lower energy data and the Maslov and JENDL-3.3 evaluations.

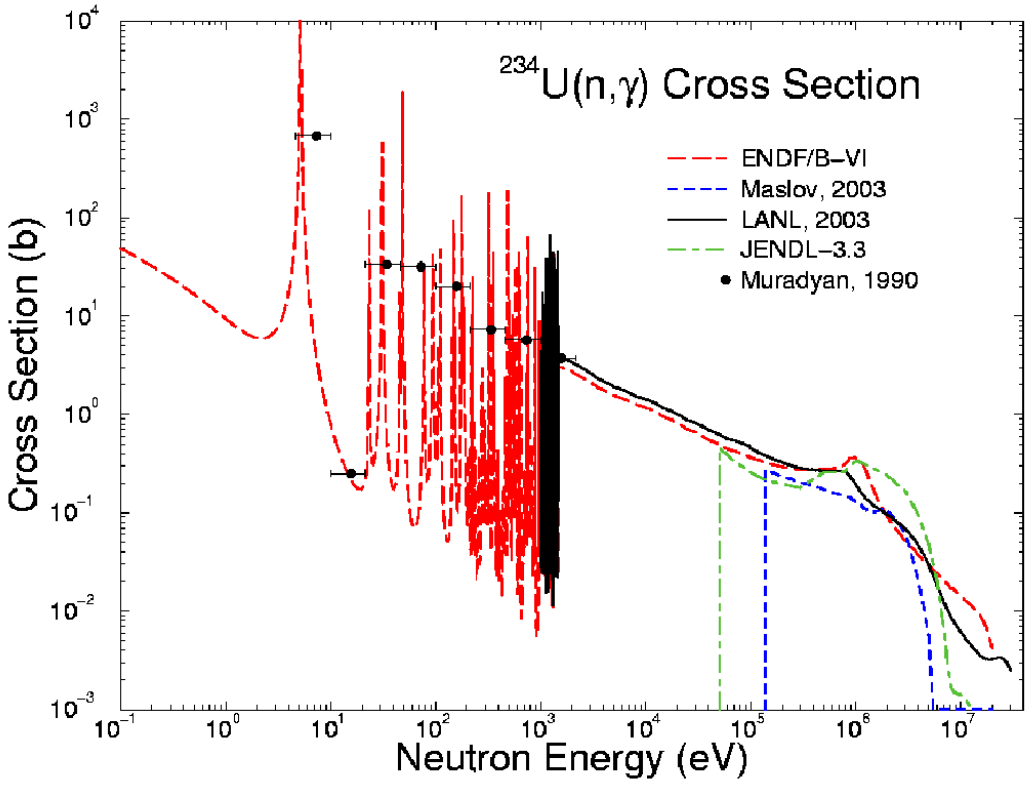

Fig. 20. Evaluated ^{234}U(n,γ) cross section from 0.01 eV to 30 MeV compared to Muradyan et al.[3] experimental data.

The total nonelastic cross section that results from summing all the individual reactions is shown between 0.2 and 2 MeV in Fig. 21 and between 2 and 30 MeV in Fig. 22. We also include in Figs. 21 and 22 the reaction cross section that results from our coupled-channels optical model calculations. Again, the reaction cross section is significantly higher than the nonelastic cross section at lower energies because it includes the compound elastic cross section. Above 2 MeV, the compound elastic is very small and the reaction cross section essentially equals the nonelastic cross section. The structure in our nonelastic cross section near 7 and 15 MeV results from structure in Behren's[29] fission cross section measurement.

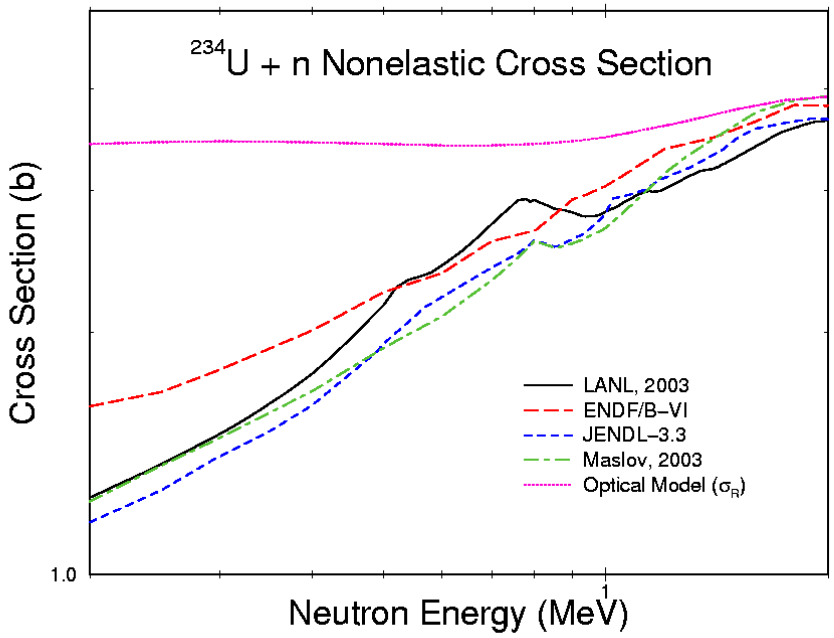

Fig. 21. Evaluated ^{234}U + n nonelastic cross section from 0.2 to 2 MeV. The optical model reaction cross section is included for comparison.

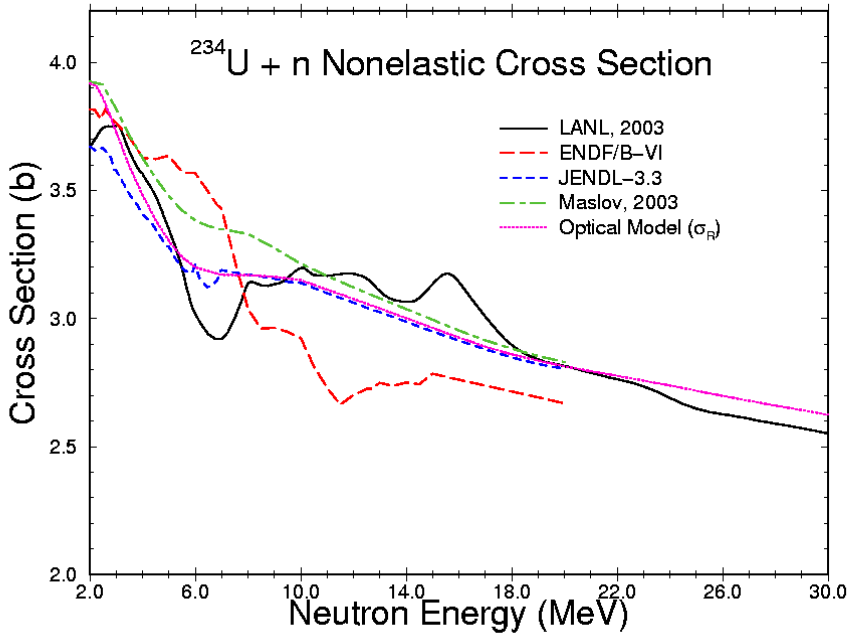

Fig. 22. Evaluated ^{234}U + n nonelastic cross section from 2 to 30 MeV. The optical model reaction cross section is included for comparison.

The neutron total cross section (MT = 1) from 100 keV to 30 MeV is based on the ECIS96 coupled channels optical model calculations. These results are compared to the other evaluations between 0.04 and 2 MeV in Fig. 23 and between 2 and 30 MeV in Fig. 24.

We obtained the elastic cross section by subtracting the nonelastic cross section from the total cross section. These results are compared to the other evaluations between 0.04 and 2 MeV in Fig. 25 and between 2 and 30 MeV in Fig. 26. We also include the shape elastic cross section from our optical model calculations in Figs. 25 and 26. The shape elastic differs from the full elastic cross section by the compound elastic cross section, so it is essentially equivalent to the elastic cross section above approximately 2 MeV. Because we utilized experimental data for the fission cross section and included (n,n') direct cross sections from our ^{238}U analysis, our evaluated elastic cross section does not exactly equal the optical model values. As seen in Fig. 26, however, the two results are reasonably close above 2 MeV. Again, some of the gross structure in the elastic cross section results from structure in Behren's experimental (n,f) data that we used in obtaining our evaluated fission cross section.

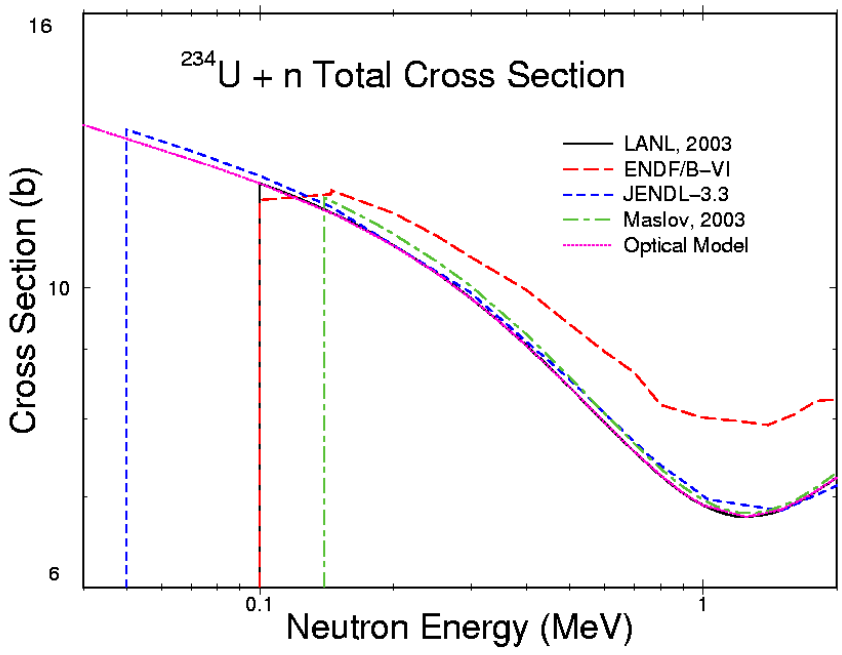

Fig. 23. Evaluated and calculated ^{234}U + n total cross section from 0.04 to 2 MeV.

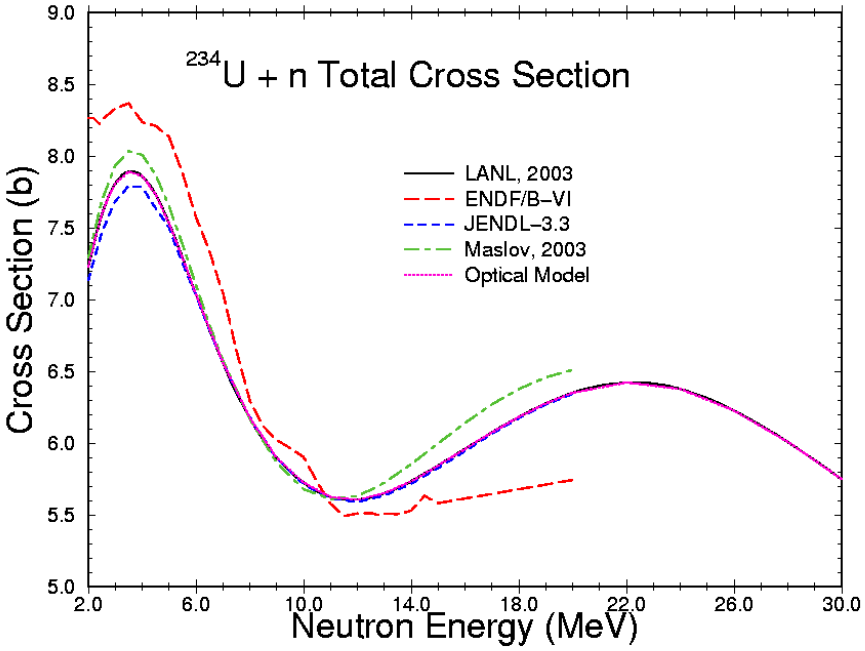

Fig. 24. Evaluated and calculated ^{234}U + n total cross section from 2 to 30 MeV.

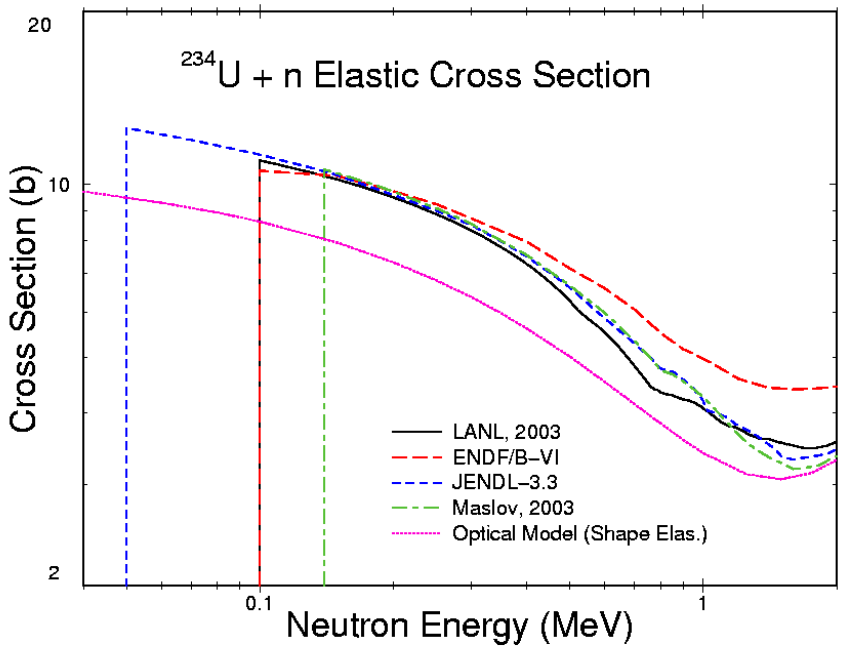

Fig. 25. Evaluated and calculated ^{234}U + n elastic cross section from 0.001 to 2 MeV.

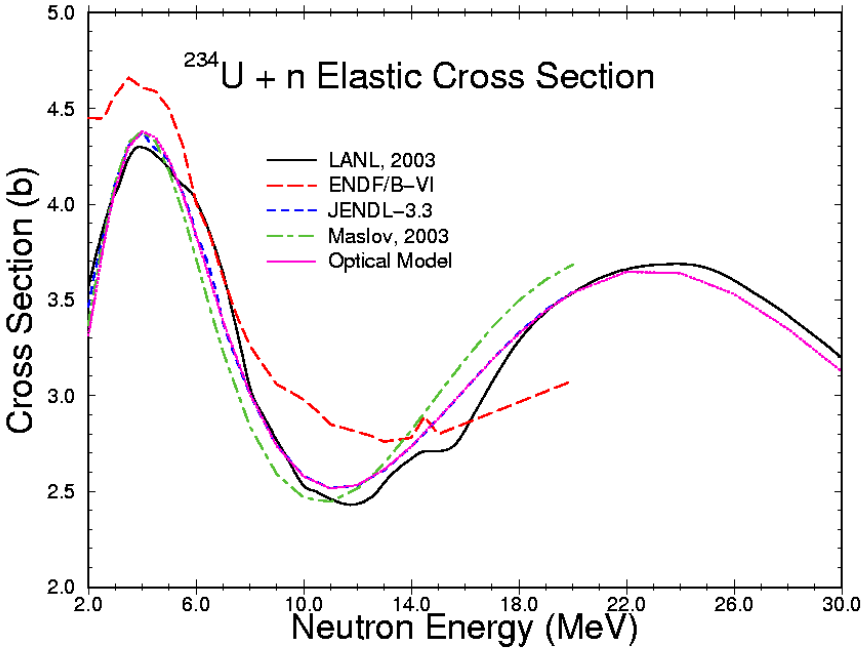

Fig. 26. Evaluated and calculated ^{234}U + n elastic cross section from 2 to 30 MeV.

Energy-Angle Distributions

Energy-angle distributions in MF=6 are used to represent neutrons from (n,n'continuum), (n,2n), (n,3n), and (n,4n) reactions, corresponding to MT=91, 16, 17, and 37, respectively. The energy distributions were obtained from the GNASH analysis. The angular distributions are given using Kalbach systematics[23] with the LAW=1, LANG=2 Kalbach-Mann option in MF=6.

Fission Neutron Spectra and Prompt Fission Nubar

The fission neutron spectra and prompt nubar in the present evaluation were adopted directly from the ENDF/B-VI (MOD 1) evaluation.[2] Our evaluation of prompt nubar is compared with the other evaluations in Fig. 27. All the nubar evaluations give quite similar results.

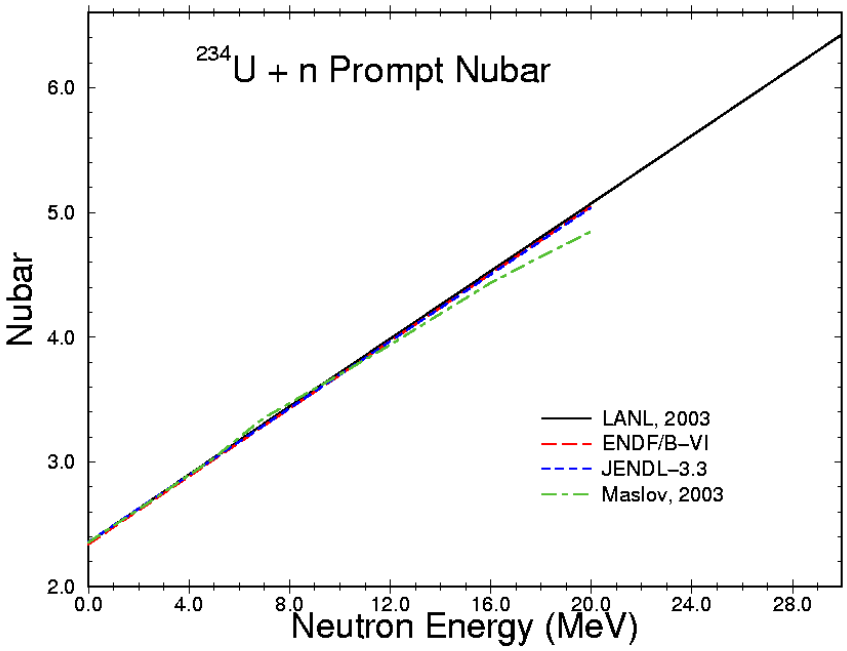

Fig. 27. Evaluated ^{234}U + n prompt fission nubar from 0 to 30 MeV

CLOSING REMARKS

We have completed new evaluations of neutron reactions on ^{232}U and ^{234}U for incident neutron energies between 10^{-5} eV and 30 MeV. The evaluations combine modern theoretical analyses with the available experimental database normalized to modern standards and are significant improvements over the previous ENDF/B-VI evaluations.

REFERENCES

[1] R. Q. Wright, T. Ohsawa, and T. Nakagawa, ^{232}U ENDF/B-VI (MOD 2) Evaluation, MAT Number 9219, National Nuclear Data Center, Brookhaven National Laboratory (Oct., 1999).

[2] M. Divadeenam, F. Mann, R. Schenter, M. K. Drake, and J. Nichols, ^{234}U ENDF/B-VI (MOD 1) Evaluation, MAT Number 9225, converted from ENDF/B-V MAT 1394 at the National Nuclear Data Center, Brookhaven National Laboratory (July, 1978).

[3] G. V. Muradyan, M. A. Voskanyan, L. P. Yastrebova, V. L. Volkov, O. Ya. Shatrov, V. I. Furman, and V. Yu. Konovalov, "Measurements of Neutron Capture Cross Sections of ^{234}U and ^{236}U and Fission Cross Section of ^{236}U," JINR-E3-98-212, 287 (1999).

[4] D. G. Madland and P. G. Young, "Neutron-Nucleus Optical Potential for the Actinide Region," Proc. Int. Conf. on *Neutron Physics and Nuclear Data for Reactors and Other Applied Purposes,*Harwell, England (pub. by OECD), p. 349 (1978).

[5] G. Haouat, J. Lachkar, Ch. Lagrange, J. Jary, J. Sigaud, and Y. Patin, *Nucl. Sci. Eng.* **81**, 491 (1982).

[6] Ch. Lagrange, "Results of Coupled Channels Calculations for the Neutron Cross Sections of a Set of Actinide Nuclei," NEANDC(E) 228L [INDC (FR) 56/L] (1982).

[7] P. G. Young and E. D. Arthur, "Calculation of ^{235}U(n,n') Cross Sections for ENDF/B-VI," Int. Conf. on *Nuclear Data for Science and Technology,* Mito, Japan, May 30 – June 3, 1988 (Ed. S. Igarasi, Saikon Publ. Co., Ltd., 1988) p. 603.

[8] P. G. Young and E. D. Arthur, "Theoretical Analyses of (n,xn) Reactions on ^{235}U, ^{238}U, ^{237}Np, and ^{239}Pu for ENDF/B-VI," Proc. Int. Conf. on *Nuclear Data for Science and Technology,* Julich, Germany, 13-17 May 1991, [Ed. S. M. Qaim, Springer-Verlag, Germany (1992)], p. 894.

[9] P. G. Young and M. B. Chadwick, "^{237,239,241}U + n Evaluations," internal memo to S. Frankle, X-5, Los Alamos National Laboratory, memo no. T-16:NW-2/10-00 (6 Oct. 2000).

[10] J. Raynal, "Notes on ECIS94," CEA Saclay Report No. CEA-N-2772 (1994).

[11] C. L. Dunford, "A Unified Model for Analysis of Compound Nucleus Reactions,"AI-AEC-12931, Atomics Int. (1970).

[12] P. G. Young, E. D. Arthur, and M. B. Chadwick, "Comprehensive Nuclear Model Calculations: Theory and Use of the GNASH Code," Proc. Workshop NUCLEAR REACTION DATA AND NUCLEAR REACTORS, ICTP, Trieste, Italy, 15 April - 17 May 1996 [Ed: A. Gandini and G. Reffo, World Scientific Publ. Co., Singapore (1998)] p. 227-404.

[13] E. D. Arthur, "Use of the Statistical Model for the Calculation of Compound Nucleus Contributions to Inelastic Scattering on Actinide Nuclei," Proc. of OECD/NEA Specialists' Meeting on *Fast Neutron Scattering on Actinide Nuclei*, (Paris, November, 1981), NEANDC-158 "U" (1982) p. 145.

[14] J. Kopecky and M. Uhl, "Test of Gamma-Ray Strength Functions in Nuclear Reaction Model Calculations," *Phys. Rev. C* **42**, 1941 (1990).

[15] A. Gilbert and A. G. W. Cameron, "A Composite Nuclear-Level Density Formula with Shell Corrections," *Can. J. Phys.* **43**, 1446 (1965).

[16] H. C. Britt, personal communication, 1982.

[17] S.F. Mughabghab, Neutron Cross Sections, Vol. 1, Part B, (Academic Press, 1984).

[18] F. M. Mann, ^{232}U ENDF/B-VI (MOD 1) Evaluation, MAT Number 9219, National Nuclear Data Center, Brookhaven National Laboratory (Oct., 1977).

[19] V. M. Maslov, Yu. V. Porodzinskij, N. A. Tetereva, A. B. Kagalenko, N. V. Kornilov, M. Baba, and A. Hasegawa, "Neutron Data Evaluation of ^{232}U," International Atomic Energy Agency, International Nuclear Data Committee report INDC(BLR)-015 (March, 2003).

[20] T. Ohsawa and T. Nakagawa, ^{232}U JENDL-3.2 Evaluation, MAT Number 9219, Japanese Atomic Energy Research Institute (March 1987).

[21] P. G. Young and M. B. Chadwick, and R. E. MacFarlane, 238U ENDF/B-VI (MOD 5) evaluation, MAT 9237, National Nuclear Data Center, Brookhaven National Laboratory.

[22] B. I. Fursov, E. Yu. Baranov, M. P. Klemyshev, B. F. Samylin, G. N. Smirenkin, and Yu. M. Turchin, *At. En*. **61**, 383 (1986); English translation: *Sov. J. At. En*. **61**, 963 (1987).

[23] C. Kalbach, "Systematics of Continuum Angular Distributions: Extensions to Higher Energies," Phys. Rev. C 37, 2350 (1988); see also C. Kalbach and F. M. Mann, "Phenomenology of Continuum Angular Distributions. I. Systematics and Parameterization," Phys. Rev. C 23, 112 (1981).

[24] G. D. James, J. W. Dabbs, J. A. Harvey, N. W. Hill, and R. H. Schindler, *Phys. Rev*. **C15**, 2083 (1977).

[25] T. Watanabe, ^{234}U JENDL-3.3 Evaluation, MAT Number 9225, Japanese Atomic Energy Research Institute (March 1987).

[26] V. M. Maslov, Yu. V. Porodzinskij, N. A. Tetereva, A. B. Kagalenko, N. V. Kornilov, M. Baba, and A. Hasegawa, "Neutron Data Evaluation of ^{234}U," International Atomic Energy Agency, International Nuclear Data Committee report INDC(BLR)-017 (March, 2003).

[27] P. Talou and P. G. Young, personal communcation, January, 2002.

[28] A. D. Carlson, S. Chiba, F. –J. Hambsch, and N. Olsson, "Update to Nuclear Data Standards for Nuclear Measurements," summary report of an IAEA Consultants' Meeting, Vienna, 2-6 December, 1996, INDC(NDS)-368 (1997).

[29] J. W. Behrens and G. W. Carlson, *Nucl. Sci. Eng*. **63**, 250 (1977).

[30] B. I. Fursov, E. Yu. Baranov, M. P. Klemyshev, B. F. Samylin, G. N. Smirenkin, and Yu. M. Turchin, *At. En*. **71**, 320 (1991).

[31] J. W. Meadows, Nucl. Sci. Eng. 65, 171 (1978).

[32] K. Kanda, H. Imaruoka, K. Yoshida, O. Sato, and N. Hirakawa, Measurement of Fast Neutron-Induced Fission Cross Sections of ^{232}Th, ^{233}U, and ^{234}U relative to ^{235}U," *Rad. Effects* **93**, 233 (1986).

[33] J. W. Meadows, *Ann. Nucl. En.* **15**, 421 (1988).

[34] R. E. MacFarlane, NJOY 99: NJOY Nuclear Data Processing System, T-2 Nuclear Information Service, http://t2.lanl.gov/codes/codes.html.